Original Article

Separately Inherited Defects in Insulin Exocytosis and β-Cell Glucose Metabolism Contribute to Type 2 Diabetes

Charlotte Granhall, Anders H. Rosengren, Erik Renström, and Holger Luthman

The effects of genetic variation on molecular functions predisposing to type 2 diabetes are still largely unknown. Here, in a specifically designed diabetes model, we couple separate gene loci to mechanisms of β-cell pathology. *Niddm1i* is a major glucose-controlling 16-Mb region in the diabetic GK rat that causes defective insulin secretion and corresponds to loci in humans and mice associated with type 2 diabetes. Generation of a series of congenic rat strains harboring different parts of GK-derived *Niddm1i* enabled fine mapping of this locus. Congenic strains carrying the GK genotype distally in *Niddm1i* displayed reduced insulin secretion in response to both glucose and high potassium, as well as decreased single-cell exocytosis. By contrast, a strain carrying the GK genotype proximally in *Niddm1i* exhibited both intact insulin release in response to high potassium and intact single-cell exocytosis, but insulin secretion was suppressed when stimulated by glucose. Islets from this strain also failed to respond to glucose by increasing the cellular ATP-to-ADP ratio. Changes in β-cell mass did not contribute to the secretory defects. We conclude that the failure of insulin secretion in type 2 diabetes includes distinct functional defects in glucose metabolism and insulin exocytosis of the β-cell and that their genetic fundaments are encoded by different loci within *Niddm1i*. *Diabetes* 55:3494–3500, 2006

Type 2 diabetes, or non–insulin-dependent diabetes, results from a combination of peripheral insulin resistance and defects in insulin secretion from the pancreatic β-cells. The genetic influence on the population variation in insulin resistance and, especially, insulin secretion is profound (1–3). Genetic susceptibility to the risk for type 2 diabetes is polygenic and highly dependent on environmental factors (4,5). Coupling of candidate genes to cellular functional defects in multifactorial diseases like type 2 diabetes is facilitated by studies of inbred animal models that have an inherited susceptibility to disease and are raised in standardized environments.

The GK rat is a widely used model for type 2 diabetes and has a well-characterized phenotype with insulin resistance, impaired insulin secretion, as well as late complications (6,7). As in humans, diabetes in the GK rat is regulated by several quantitative trait loci (8,9). The *Niddm1i* locus is a glucose-controlling locus that has been investigated in the congenic strain NIDDM1I. The NIDDM1I rat, harboring a 16-Mb GK-derived genome segment on chromosome 1, demonstrates hyperglycemia combined with defects in insulin secretion from the pancreatic β-cells (10,11). Genetic data from humans (chromosome 10q24-26) and mice (chromosome 19) indicate that *Niddm1i* is a species-conserved diabetes susceptibility locus (12–14). Recent studies have identified two genes within *Niddm1i* associated with diabetes in mice (*Sorcs1*) and humans (*Tcf7l2*) (15,16). Here, to further dissect the functional and genetic components of inherited insulin secretion defects, we have generated five subcongenic strains harboring different parts of the *Niddm1i* locus. We combine this genetic approach with detailed cell-physiological investigations to identify the exact nature of the defects underlying reduced insulin release. This approach enabled us to identify two distinct diabetes susceptibility loci encoding impairment of pancreatic β-cell metabolism and the very process of insulin exocytosis.

RESEARCH DESIGN AND METHODS

All strains were maintained by sister-brother mating. The nondiabetic F344/DuCrl2Swe rats were originally purchased from Charles River Laboratories (Wilmington, MA). Diabetic GK/Swe rats were originally from Kyoto University. Transfer of GK alleles onto the genome of F344 rats by repeated backcrossing (10 generations) established the homozygous congenic strain F344.GK-*Niddm1i* (NIDDM1I), which carries 0.6% of the GK genotype on a homozygous F344 genetic background. Backcrossing was arranged to introduce mitochondrial DNA and sex chromosomes from F344.

The congenic strains N1IREC6, N1I12, N1I3, N1IREC1, and N1IREC11 were established from an F2 intercross between F344 and NIDDM1I, where animals with critical recombinations were selected for sister-brother breeding. F344 and congenic NIDDM1F, harboring the F344 genotype in the entire NIDDM1I region (17), display the same insulin secretion phenotype (11). NIDDM1F was used as control in the electrophysiological experiments and F344 in all other experiments. To avoid effects of the estrus cycle and other minor sex-specific influences, only males were included in this study. Rats were maintained at a constant temperature and humidity in a 12-h light/dark cycle with free access to standard laboratory chow and water. The local ethics committees approved all experiments.

Genome and genotype analysis. Genomic DNA was extracted from ear or tail biopsies by standard methods. Genetic markers were selected from public databases and in-house information and were mapped within *Niddm1i* (8). Eight new microsatellite markers (*D1Swe1-8*; available from RatMap online at http://ratmap.gen.gu.se/) were added in regions lacking informative markers. PCR amplification was performed with one primer in each pair labeled with HEX or FAM fluorescence tags (DNA Technology, Aarhus, Denmark); the products were separated on an ABI 3100 genetic analyzer (Applied Biosystems, Foster City, CA).

Histological examination. Pancreata from three rats per strain were fixed in paraformaldehyde, embedded in paraffin, sectioned (5 μm), and immuno-

From the Department of Clinical Sciences, Lund University, Malmö, Sweden.

Address correspondence and reprint requests to Holger Luthman or Erik Renström, Lund University, Department of Clinical Sciences, Malmö, CRC, Bldg. 91, Fl. 11, Entrance 72, UMAS, SE-205 02 Malmö, Sweden. E-mail: holger.luthman@med.lu.se or erik.renstrom@med.lu.se.

Received for publication 9 June 2006 and accepted in revised form 6 September 2006.

C.G. and A.H.R. contributed equally to this study.

α-KIC, sodium-4-methyl-2-oxovalerat; K_{ATP} channel, ATP-sensitive K^+ channel.

DOI: 10.2337/db06-0796

stained with an anti-insulin antibody (Jackson ImmunoResearch, West Grove, PA). Nuclei were counterstained with hematoxylin. The number and size of islets in each pancreas was counted in 3–4 sections separated by at least 40 sections. Quantitative evaluation of β-cell mass was performed using computer-assisted image analysis and an Olympus microscope, calculating the ratio between the area occupied by immunoreactive cells and the total area occupied by pancreatic cells in the section. The areas of insulin-positive cells were measured in least 50 islets from each strain with an area >5,000 μm^2.

Pancreatic RNA and protein content. Pancreatic RNA (six pancreata per strain) and RNA from islets (six rats per strain) were prepared using TRIzol reagent (Invitrogen, Stockholm, Sweden). Insulin, glucagon, and *Tcf7l2* RNA levels were determined by quantitative real-time PCR on an ABI7900 (Applied Biosystems) with cyclophilin B and *Hprt* as standards. The following gene-specific primer pairs and probes were used: *Ins1*: forward 5′-CAGCAAGCAG GTCATTGTTC-3′, reverse 5′-CCTGGGCAGGCTTGG-3′, probe 5′-CTTCCTGC CCCTGCTGGCC-3; *Tcf7l2*: forward 5′-TCAATGAATCAGAGACGAATCAAAA C-3′, reverse 5′-TTGGCCGCTTCTTCCAAAC-3′, probe 5′-CTCCTCCGATTCC GAGGCGGAAA-3′; and glucagon Rn00562293_m1 Assay-On-Demand from Applied Biosystems. Total pancreatic insulin content was determined from homogenized pancreas (six per strain) extracted by acidic-alcohol (75% ethanol) using an ELISA kit (Mercodia, Uppsala, Sweden). Total protein content was determined by measuring the absorbance at 260 nm (A_{260}) and 280 nm (A_{280}), using the Warburg formula: 1.55 A_{280} − 0.76 A_{260}= mg/ml of protein.

In vitro insulin release in islets. Isolated pancreatic islets were prepared by collagenase digestion, handpicked, and incubated in a humidified atmosphere in RPMI 1640 tissue culture medium (SVA, Uppsala, Sweden) with 5 mmol/l glucose and supplemented with 10% (vol/vol) FCS, 100 IU/ml penicillin, and 100 μg/ml streptomycin. After overnight incubation at 37°C, the islets were preincubated for 30 min in Krebs-Ringer bicarbonate buffer with 0.1% BSA and 3.3 mmol/l glucose. After preincubation, the buffer was changed to a medium containing the agents to be tested, and triplicates of 10 islets were incubated for 60 min. Insulin levels were measured by radioimmunoassay after incubation with 3.3 mmol/l glucose, 20 mmol/l glucose, 50 mmol/l K^+, 2 μmol/l glybenclamide, and 20 mmol/l sodium-4-methyl-2-oxovalerat (α-KIC).

Islet cell preparation. Single β-cells were prepared by shaking islets in a Ca^{2+}-free medium as previously described (18). The resultant cell suspensions were plated on plastic Petri dishes and incubated for up to 2 days, as specified above.

Electrophysiology. Plastic Petri dishes were used as the experimental chamber with a plastic insert to reduce the volume to ~0.5 ml. The dish was continuously perfused at a rate of 2 ml/min at 31–33°C. Patch pipettes were pulled from borosilicate glass, coated with Sylgard, and fire polished to an average resistance of 4–6 MΩ when filled with pipette solution. The zero-current potential of the pipette was adjusted with the pipette in the bath. Whole-cell capacitance measurements were performed using an EPC-10 patch-clamp amplifier with PULSE software (version 8.64; HEKA, Lambrecht-Pfalz, Germany). β-Cells were identified based on their size and the inactivation properties of the voltage-gated Na^+ currents (19,20). Exocytosis was detected as increases in cell capacitance, using the "Sine + DC" mode of the lock-in amplifier included in the PULSE software and the standard whole-cell configuration. When eliciting exocytosis, a train of 10 500-ms depolarizations from −70 to 0 mV was applied. The extracellular solution consisted of (in mmol/l): 118 NaCl, 20 TEACl (tetraethylammonium chloride), 5.6 KCl, 2.6 $CaCl_2$, 1.2 $MgCl_2$, 5.0 HEPES, and 5.0 glucose (pH 7.4 with NaOH). The pipette solution contained (in mmol/l): 125 Cs-glutamate, 10 CsCl, 10 NaCl, 1.0 $MgCl_2$, 5.0 HEPES, 50 μmol/l EGTA, 3.0 μmol/l ATP, and 0.1 μmol/l cAMP (pH 7.2 with CsOH).

Mitochondrial membrane potential. Mitochondrial membrane potential was measured by Rh123 fluorescence (21). Freshly isolated islets were incubated with 13 μmol/l Rh123 (Sigma-Aldrich, Stockholm, Sweden) for 30–60 min in Hanks' balanced salt solution (Sigma-Aldrich), supplemented with 4.1 mmol/l $NaHCO_3$. On investigation, a single islet was transferred to a separate glass-bottomed dish containing 1,000 μl Hanks' balanced salt solution and placed on the heated and gas-equilibrated (37°C, 95% air/5% CO_2) microscope stage (Carl Zeiss, Germany). Time-lapse images were recorded every 20 s. Rh123 fluorescence was excited using the 488-nm line of a krypton-argon laser of a Zeiss LSM 510 META confocal microscope, and emitted light was collected via a Zeiss Plan-Apochromat 10× objective, using a band-pass 526- to 537-nm filter. The pinhole was maximized, resulting in a confocal section thickness of 140 μm. Rh123 fluorescence intensity was measured from the entire islet for each image frame. The osmolarity of the solutions remained constant throughout the experiment.

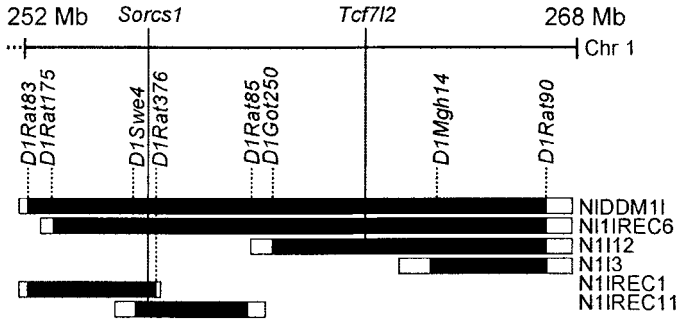

FIG. 1. Congenic strains within *Niddm1i*. The filled bars designate known homozygous GK segments; the open ends designate intervals containing the recombinant end points. The positions of the genes *Sorcs1* and *Tcf7l2* are indicated. The locations of markers and genes were taken from Ensembl Rattus Norvegicus version 40.34j based on RGSC 3.4 (available from http://www.ensembl.org) determined according to release 33.34c from ENSEMBL, based on NCBI assembly 3.4 of the rat genome. The figure is drawn to scale. Chr, chromosome.

ATP-to-ADP ratio. Adenosine nucleotides (ATP and ADP) were assessed by luminometric determination of the luciferin-luciferase reaction using an SL ATP kit (BioThema, Handen, Sweden). Islets were isolated and incubated in culture medium overnight. Islets were preincubated for 30 min in Krebs buffer, and triplicates of 10 islets were incubated at 37°C for 5 min in 300 μl of 3.3 or 20 mmol/l glucose. After incubation, 30 μl trichloacetic acid (20%) was added, and the samples were vortexed for 20 s and fast frozen in alcohol on dry ice. Samples were stored at −80°C until assayed for ATP on a Wallac Victor 1420 multilable counter. ADP concentrations were measured after depletion of endogenous ATP with ATP sulfurylase, followed by ADP conversion to ATP and luminometric determination. Data are presented as the ATP-to-ADP ratio, making them independent of islet size or loss of sample volume during extraction.

Statistical analysis. Data are the means ± SE. Statistical significance was evaluated using the two-tailed unpaired Student's *t* test.

RESULTS

Congenics within *Niddm1i* display normal islet architecture and β-cell mass. In all strains (Fig. 1), pancreatic β-cells were located in the center of the islets, and the α-cells formed a peripheral crown (data not shown). We estimated the β-cell mass by morphometric counting and found no significant differences in the ratio between islet area and the total area occupied by pancreatic cells (Table 1). The number of β-cells per islet in the congenic strains was comparable to control, as was the wet weight of the

TABLE 1
Characterization of pancreata

	Control	NIDDM1I	N1IREC6	N1I12	N1I3	N1IREC1	N1IREC11
Pancreas weight (mg)	875 ± 29	906 ± 24	882 ± 38	846 ± 19	886 ± 24	845 ± 21	850 ± 19
Insulin content (ng insulin/mg protein)	204 ± 21	231 ± 18	207 ± 21	299 ± 20*	239 ± 33	199 ± 23	196 ± 25
Islet area/total pancreatic area (%)	1.28 ± 0.12	1.27 ± 0.13	1.45 ± 0.13	1.08 ± 0.08	1.07 ± 0.12	1.23 ± 0.14	1.26 ± 0.11
β-Cell area/islet area (%)	61.1 ± 1.1	61.8 ± 1.2	58.7 ± 1.1	59.7 ± 1.1	57.4 ± 1.2†	60.2 ± 1.2	60.4 ± 1.1
Insulin RNA level (relative expression)	1.08 ± 0.06	1.21 ± 0.07	1.16 ± 0.05	1.13 ± 0.09	1.23 ± 0.05	0.98 ± 0.05	1.27 ± 0.07
Glucagon RNA level (relative expression)	1.26 ± 0.07	1.44 ± 0.09	1.56 ± 0.12	1.35 ± 0.08	1.40 ± 0.05	1.28 ± 0.06	1.59 ± 0.08†

Data are the means ± SE. *P* values denote comparison between congenic strain and control. *$P < 0.01$; †$P < 0.05$.

TABLE 2
Insulin release in isolated pancreatic islets

	Control	NIDDM1I	N1IREC6	N1I12	N1I3	N1IREC1	N1IREC11
3.3 mmol/l glucose	0.09 ± 0.03	0.12 ± 0.04	0.10 ± 0.02	0.21 ± 0.05*	0.22 ± 0.07	0.21 ± 0.05*	0.11 ± 0.04
20 mmol/l glucose	2.23 ± 0.10	0.87 ± 0.16†	1.01 ± 0.21†	1.19 ± 0.12†	1.95 ± 0.22	1.26 ± 0.12†	1.81 ± 0.24
20 mmol/l α-KIC	4.13 ± 0.40	2.89 ± 0.30*	2.82 ± 0.36*	3.17 ± 0.28	3.26 ± 0.54	3.61 ± 0.36	3.70 ± 0.69
20 μmol/l glybenclamide	1.17 ± 0.18	0.64 ± 0.09*	0.56 ± 0.11‡	0.65 ± 0.21	0.95 ± 0.21	0.87 ± 0.16	1.01 ± 0.13
50 mmol/l K^+	1.12 ± 0.16	0.63 ± 0.05*	0.81 ± 0.16	0.66 ± 0.07*	1.03 ± 0.10	0.90 ± 0.24	1.17 ± 0.19

Data are the means ± SE (in ng insulin · $islet^{-1}$ · h^{-1}, n = 4–8 rats per strain). P values <0.05 are indicated and denote comparison between congenic strain and control. *$P < 0.05$; †$P < 0.001$; ‡$P < 0.01$.

pancreata. The insulin protein content was similar to control in all congenic strains except N1I12, which exhibited 47% higher insulin levels than control (Table 1). However, pancreatic insulin RNA levels were similar in all strains, including control. Glucagon levels were also equal in all strains, except for N1IREC11, which displayed 26% higher levels than control. Overall, these results indicate that the GK genotype within *Niddm1i* does not influence islet architecture or β-cell mass to any major extent, suggesting that the defect in insulin secretion was a consequence of loss of β-cell function, rather than disturbed β-cell differentiation.

Impaired insulin secretion in isolated islets from the NIDDM1I, N1IREC6, N1I12, and N1IREC1 congenic strains. The mechanisms coupling an elevation in blood glucose to β-cell electrical activity are fairly well characterized (22). When glucose is metabolized through glycolysis and the mitochondrial Krebs cycle of the β-cell, ATP is generated. The intracellular rise in the ATP-to-ADP ratio leads to closure of the β-cell ATP-sensitive K^+ channels (K_{ATP} channels), followed by calcium influx and exocytosis of insulin-containing granules. To define and locate the mechanistic defect within *Niddm1i*, insulin secretion studies were performed in batch-incubated islets from NIDDM1I and subcongenic strains. The islets were treated with either low (3.3 mmol/l) or high (20 mmol/l) glucose, the mitochondrial substrate α-KIC, the K_{ATP} channel inhibitor glybenclamide, or high potassium to directly depolarize the β-cell. For glucose-evoked insulin secretion, the most pronounced difference was observed between control and the NIDDM1I strain (with the GK genotype in the complete 16-Mb *Niddm1i* region), showing a 61% reduction of insulin secretion compared with control ($P < 0.001$) (Table 2). Insulin release was also suppressed by 55% in the N1IREC6 strain, which carries the GK genotype in the complete region, save for 1 Mb in the most proximal part of *Niddm1i*. The N1IREC1 strain, which carries the 4-Mb GK genotype proximally in *Niddm1i*, demonstrated a 54% decrease in insulin secretion ($P < 0.001$), and N1I12, which carries the 8.7-Mb GK genotype in the distal part of *Niddm1i*, showed a 47% reduction in insulin secretion ($P < 0.001$). Interestingly, two congenic strains exhibited normal responses to glucose. Neither N1I3, carrying the 4.2-Mb GK genotype most distal in *Niddm1i*, nor N1IREC11, with the 3.8-Mb GK genotype in the middle part of *Niddm1i*, showed any signs of impaired insulin secretion in isolated islets. The segment of the GK genotype (3 Mb) differing between N1IREC1 and N1IREC11 in the most proximal part of *Niddm1i* was thus responsible for the impaired insulin secretion in N1IREC1, whereas the segment of the GK genotype (4.5 Mb) differing between N1I12 and N1I3 in the distal part of *Niddm1i* was responsible for the reduced insulin secretion in N1I12. The effect of other secretagogues was also investigated. NIDDM1I displayed significantly impaired insulin secretion in response to α-KIC (30%), glybenclamide (45%), and high potassium (50%). The same trends were seen in N1IREC6 and N1I12. N1IREC1, however, did not have impaired secretion in response to any secretagogues other than glucose.

Impaired single-cell exocytosis in NIDDM1I, N1IREC6, and N1I12 strains. Single β-cell exocytosis was monitored as increases in whole-cell membrane capacitance (Fig. 2*A*). Exocytosis was triggered by a train of 10 depolarization pulses from the holding potential −70 to 0 mV applied at 1 Hz (Fig. 2*B*). The total capacitance increase (ΔC_{tot}) in control β-cells amounted to 113 ± 13 fF (n = 13) (Fig. 2*C*). N1I3 β-cells (4.2-Mb GK genotype distal in *Niddm1i*) demonstrated a similar exocytotic response. Furthermore, there was no significant difference between the N1IREC11 strain (n = 41) and control (not shown). However, in excellent agreement with the islet insulin release measurements, exocytosis in the NIDDM1I (complete *Niddm1i* region) and N1I12 (8.7-Mb GK genotype distal in *Niddm1i*) strains was markedly reduced. The total capacitance increase in the NIDDM1I strain was 63 ± 6 fF, which is 45% less than in control β-cells (n = 19 for NIDDM1I, $P < 0.01$), and exocytosis was reduced by 49% in the N1I12 strain (n = 21 for N1I12, $P < 0.001$). Moreover, exocytosis in the N1IREC6 strain, with the GK genotype in the complete region save for the most proximal part of *Niddm1i*, amounted to 65 ± 8 fF (n = 21, $P <$ 0.01 vs. control) (data not shown). Interestingly, the N1IREC1 strain (4-Mb GK genotype proximal in *Niddm1i*) showed 35 and 50% enhanced exocytotic capacity (87 ± 8 fF, n = 33) compared with NIDDM1I ($P < 0.05$) and N1I12 ($P < 0.01$) strains, respectively. As described above, N1IREC1 islets revealed impaired insulin release after high-glucose challenge, whereas insulin secretion in response to high [K^+] (the condition most related to voltage-clamp depolarization) was in the same range as control islets (Table 2). Taken together, the cell capacitance and measurements of insulin release indicate that the N1IREC1 strain, albeit deteriorated in glucose-stimulated insulin secretion, retains a more well-functioning exocytotic machinery than the N1I12 and NIDDM1I strains.

Impaired mitochondrial function in the N1IREC1 strain. Mitochondrial membrane potential was assessed using the potentiometric dye Rh123. Elevation of the glucose concentration from 1 to 20 mmol/l resulted in mitochondrial hyperpolarization, as evidenced by the average 7.7 ± 0.5% (n = 46) reduction in fluorescence in control islets (Figs. 3*A* and *B*). The fluorescence in NIDDM1I islets decreased by 6.4 ± 0.8% (not significant versus control). Intriguingly, fluorescence intensity in the N1IREC1 strain decreased by 9.5 ± 0.7% (n = 12) on glucose addition. This decrease was 25% more pronounced

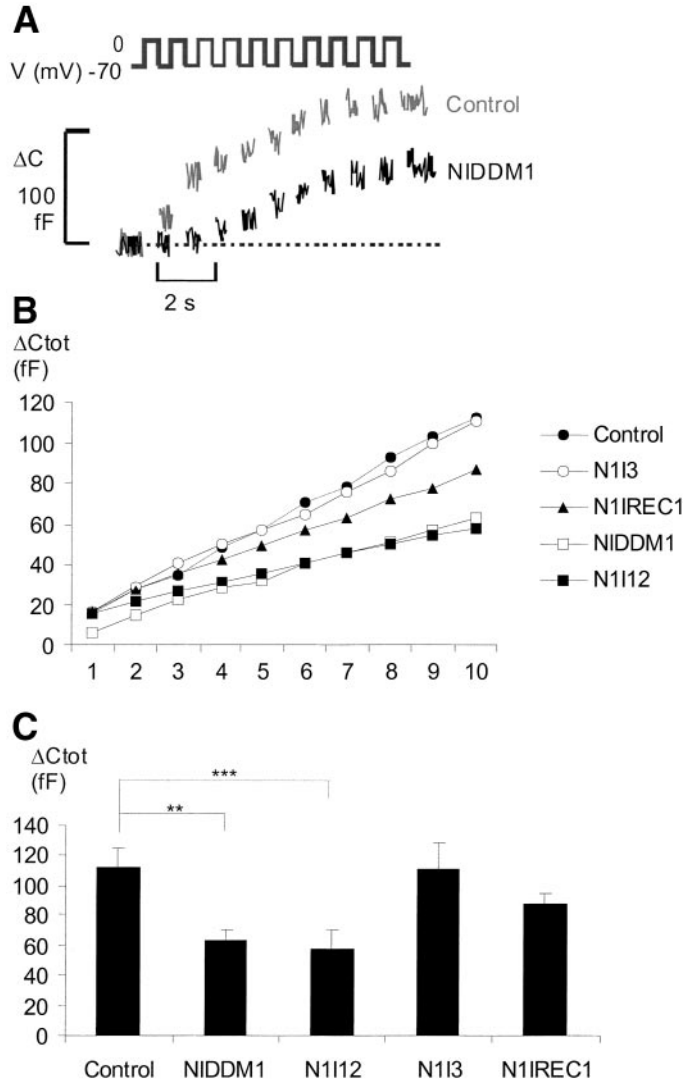

FIG. 2. Single β-cell exocytosis in different *Niddm1i* congenic strains. *A*: Exocytosis evoked by trains of 10 depolarizations (V) and monitored as increases in cell capacitance (ΔC) in control (gray) and NIDDM1I (black) β-cells. *B*: Average accumulated capacitance increase (ΔCtot) elicited by trains of depolarizations in β-cells from different congenic strains as depicted. Error bars are omitted in this figure for reasons of clarity. *C*: ΔCtot evoked by the entire train. Data are the mean values ± SE in 13 control, 19 NIDDM1I, 21 N1I12, 15 N1I3, and 33 N1IREC1 β-cells. **$P < 0.01$; ***$P < 0.001$.

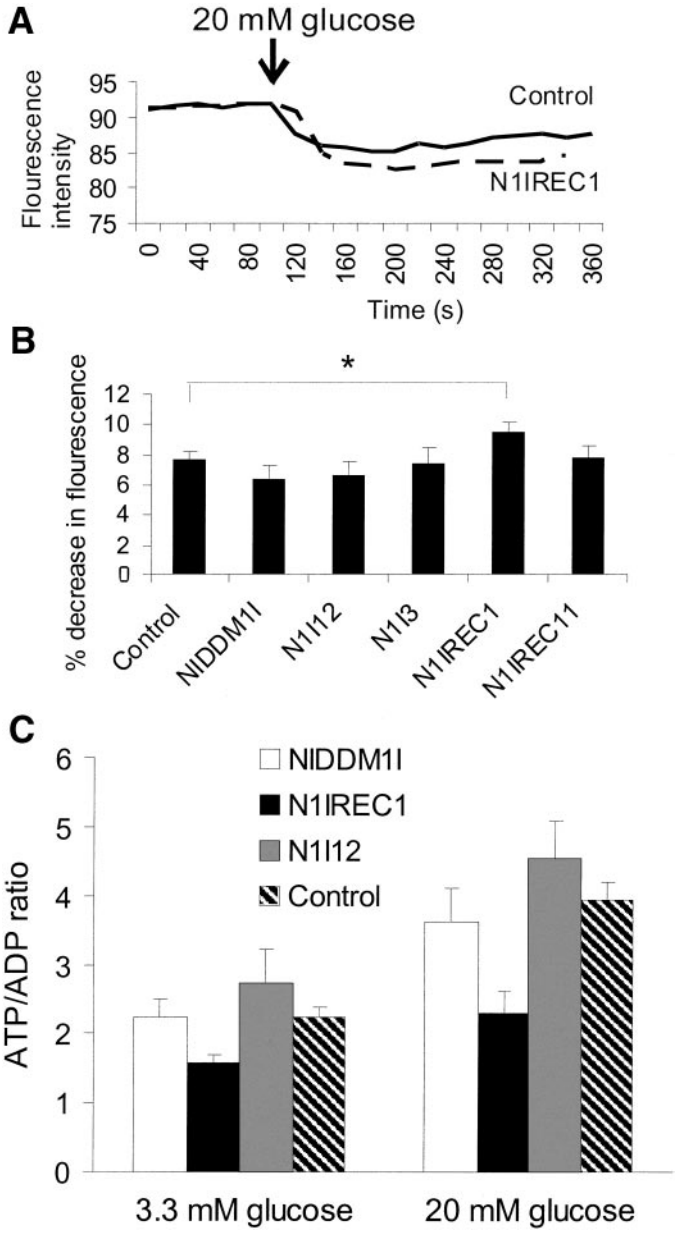

FIG. 3. Mitochondrial membrane potential and ATP production. *A*: Time-lapse images of Rh123 fluorescence intensity (arbitrary units) in a single control (solid line) and N1IREC1 (dashed line) islet. Before the experiment, islets were incubated in 13 μmol/l Rh123 and 1.0 mmol/l glucose, followed by stimulation with 20 mmol/l glucose, as indicated. A decrease in fluorescence intensity reflects mitochondrial hyperpolarization. *B*: Average percent decrease in Rh123 fluorescence on elevation of the glucose concentration from 1.0 to 20 mmol/l. Data are the mean values ± SE in 46 control islets, 19 NIDDM1I islets, 6 N1I12 islets, 15 N1I3 islets, 12 N1IREC1 islets, and 15 N1IREC11 islets. *$P < 0.05$. *C*: ATP-to-ADP ratio in islets after incubation in 3.3 or 20 mmol/l glucose. Data are the mean values ± SE in four to five experiments (= animals)/strain. **$P < 0.01$.

than in controls ($P < 0.05$). Islets from the other strains responded in a manner similar to the control islets. Because the increase in the ATP-to-ADP ratio is fundamental to initiation of β-cell electrical activity and insulin secretion, we next examined the cytosolic adenine nucleotide levels. In control islets, the ATP-to-ADP ratio increased from 2.2 at low glucose to 3.6 at high glucose concentration (Fig. 3*C*). Similar glucose-evoked stimulation of ATP-to-ADP was observed for the NIDDM1I and N1I12 strains. By contrast, the N1IREC1 strain, which only displayed impaired insulin secretion when stimulated with glucose in islet batch incubations, revealed a markedly lower ATP-to-ADP ratio compared with control. The ATP-to-ADP ratio in N1IREC1 islets was 1.6 (70% of control, $P < 0.01$) at low glucose (3.3 mmol/l) and increased to 2.3 (58% of control, $P < 0.01$) after stimulation with 20 mmol/l glucose. This corresponds to a 1.4-fold increase in the ATP-to-ADP ratio in islets from the N1IREC1 strain on glucose elevation, which is significantly less than the 1.75-fold increase in the ATP-to-ADP ratio observed in control rats in response to glucose ($P < 0.05$). This finding, together with the observation that islets from the N1IREC1 strain exhibited aberrant mitochondrial hyperpolarization, GK genotype in the 3-Mb proximal region of *Niddm1i* encodes impaired glucose metabolism.

Expression of *Tcf7l2*. Determination of *Tcf7l2* RNA levels in islets revealed higher RNA levels in diabetic GK rats (3.1-fold overexpression compared with control), but

there was no evidence of *Tcf7l2* differences between congenic N1I12 rats that contain the GK allele for *Tcf7l2* and control rats (data not shown).

DISCUSSION

In this study, we dissected the functional consequences of diabetes-associated genetic variations in the major species-conserved diabetes susceptibility locus *Niddm1i*. Using congenic rat strains derived from the spontaneously diabetic GK rat and a combination of histological methods, in vitro hormone release assays, cell physiology, and biochemistry, we demonstrate that the *Niddm1i* locus confers a defect in insulin secretion. This is not caused by a reduction in β-cell mass, but rather by a deteriorated function of the individual β-cell. The functional β-cell defect can in turn be divided into two distinct categories: general malfunction of Ca^{2+}-dependent insulin exocytosis and impaired glucose metabolism, which are encoded by different subloci within *Niddm1i*.

Advantages of the congenic animal model. The capacity for insulin secretion is a genetically inheritable trait. Defective insulin secretion is a central feature of the rare monogenic forms of diabetes (e.g., MODY [maturity-onset type of diabetes in the young]) (23), but it is also important for "classical" type 2 diabetes (24). Development of the latter much more common form of diabetes involves variations in a large number of genes, the identities of which remain poorly elucidated. Unraveling the polygenic nature of type 2 diabetes has proved very cumbersome in humans. This is in part attributable to confounding variations in environmental factors, which also are crucial for the development of disease. These environmental factors can be better controlled if reverting to animal models of type 2 diabetes. However, to ensure that the extracted information is relevant for the understanding of human disease, it is essential that the animal model used harbors naturally occurring genetic variations in loci that are conserved among species. In both of these respects, the GK rat-derived *Niddm1i*-congenic animal model represents a major advance. First, avoiding manipulation of genomic DNA circumvents possible artifacts that are associated with common transgenic techniques (25). Second, the *Niddm1i* locus, located at the telomeric end of chromosome 1 in the GK rat, is also a type 2 diabetes susceptibility locus in humans and corresponds to human chromosome 10q24-q26 (12,16). Furthermore, unique to this model is the possibility to combine mechanistic information about cellular defects with genetic information that can be honed down to limited sets of genes, making the combined identification of candidate genes and cellular malfunction in diabetes a realistic feat. The fact that the congenic rats at the age of investigation (60 days) had not developed overt type 2 diabetes means that the β-cell phenotype was not the result of severe hyperglycemia. Interestingly, the 61% reduction in glucose-induced insulin secretion in the NIDDM1I strain (Table 2) was similar to the 60–70% reduction typically observed in islets from the GK rat (26), which underlines the importance of the Niddm1i locus for the diabetic GK phenotype. In short, we regard this animal model approach as currently the best for extracting detailed information about which cellular functions involved in the pathophysiology of type 2 diabetes can be caused by naturally occurring genetic variations.

Pancreatic β-cell mass is intact in *Niddm1i* subcongenics. The defects in insulin secretion occurring at the onset of type 2 diabetes can be caused by a wide variety of different mechanisms. These can be roughly grouped into those that cause an absolute reduction in pancreatic β-cell mass and those that result in malfunction of the individual β-cell (27,28). A decrease in pancreatic β-cell mass may be the result of factors such as disturbed pancreatic development, reduced β-cell regeneration, or increased apoptosis (29). However, the observation that total pancreatic mass, relative β-cell area, and insulin expression at both the mRNA and protein levels remain largely unchanged, in all congenic strains (Table 1) indicates that genetic variations in the *Niddm1i* locus do not translate into defects in any of the mechanisms that control pancreatic β-cell formation or turnover. In contrast, the observation that exocytosis in individual pancreatic β-cells is suppressed in several of the congenic strains indicates functional defects at the level of the single β-cell (Fig. 2).

Functional defects in pancreatic β-cell metabolism and exocytosis. It is well known that in certain cases of type 2 diabetes, the pancreatic β-cells may contain high amounts of insulin but are unable to release the hormone into the circulation (27), which clearly suggests an impairment of the stimulus-secretion coupling of glucose-evoked insulin secretion. This can occur at any step in the sequence of reactions involved in triggering insulin secretion in the pancreatic β-cell. Glucose-evoked changes upstream of K_{ATP} channel closure include glucose transport into the β-cell, processing via glycolysis, mitochondrial metabolism, and oxidative phosphorylation. An isolated defect in any of these reactions leads to impaired glucose-evoked insulin secretion. However, this defect will be overruled if insulin secretion is directly stimulated using depolarizing concentrations of high K^+. This is exactly what was observed in the N1IREC1 congenic strain located in the proximal part of *Niddm1i* (Figs. 1 and 2, Table 2). In this particular strain, glucose indeed failed to significantly increase the intracellular ATP-to-ADP ratio (Fig. 3*C*), despite strong mitochondrial hyperpolarization (Fig. 3*A–B*). The exact site of this metabolic defect remains to be elucidated.

If the encoded functional β-cell defect instead involves the basic properties of the exocytotic release machinery, then insulin release elicited by depolarization with high K^+ is expected to be severely affected. This was seen in congenic strains NIDDM1I (covering the entire *Niddm1i* locus) (Fig. 1) and N1I12 (covering the distal 8 Mb of the *Niddm1i* locus) (Figs. 1 and 2, Table 2). Furthermore, such a genetically encoded defect in exocytosis cannot be rescued by intact glucose metabolism; this explains why glucose-evoked insulin release in N1I12 islets is suppressed.

Different gene loci are responsible for defects in β-cell metabolism and exocytosis. When combining genetic information and details of β-cell phenotypes in the different congenic strains, a careful interpretation suggests a 3-Mb dysmetabolic sublocus in the GK rat genome located proximally in *Niddm1i* (the proximal part of N1IREC1 that differs from N1IREC11) to encode defective ATP production. The data are suggestive of ATP synthase itself not being fully operational, since mitochondrial hyperpolarization appears intact (Fig. 3*A*). This dysmetabolic sublocus contains 28 known genes. Most likely the proximal limit for this locus can be further narrowed down to the proximal end of N1IREC6. In this scenario, only 12 candidate genes remain within the locus.

Located distally in *Niddm1i* is a 4.5-Mb sublocus (the region differing between N1I12 and N1I3) that encodes a more profound exocytotic defect. This is not merely attributable to decreased insulin production (Table 1) but appears to represent a truly sluggish exocytotic response to elevations in cytoplasmic Ca^{2+}. It can be speculated that this may be related to imprecise protein trafficking between membrane compartments because of aberrant expression of an exocytotic SNARE (*N*-ethylmaleimide–sensitive factor attachment protein receptor) fusion protein that is encoded by 1 of the 26 known genes in that region. Interestingly, the gene encoding for transcription factor *TCF7L2* is also located in this locus and has recently been identified as a candidate gene for type 2 diabetes in humans (16). The gene product is known to be important in the *Wnt* signaling pathway and is believed to be important for preproglucagon expression. However, *Tcf7l2* RNA levels were not different in the N1I12 strain compared with controls.

Implications for the understanding of human type 2 diabetes. Unraveling the genetic factors involved in polygenic type 2 diabetes in human has met with several problems. So far, relatively few candidate genes for human type 2 diabetes have been unequivocally identified (30). Moreover, identification of a diabetes-associated polymorphism in a candidate gene represents only the first step; after this follows an arduous task to verify the exact biological consequences. For some polymorphisms evidence for a β-cell phenotype exist, e.g., for the genes encoding for the Ca^{2+}-sensitive protease calpain 10 (31), as well as the K_{ATP} channel subunits *KIR6.2* (32) and *SUR1* (33,34). The current study combines identification of a limited set of putative candidate genes with a thorough understanding of the pathophysiological consequences. This represents an important piece of knowledge to bridge the gap between understanding the inheritance of type 2 diabetes and designing novel tailor-made therapies.

ACKNOWLEDGMENTS

This study would not have been possible without support from the EFSD (European Foundation for the Study of Diabetes), Swedish Research Council Grants 09109 (to H.L.) and 12239 (to E.R.), the Swedish Diabetes Association, the Faculty of Medicine at Lund University, Malmö University Hospital, MAS Stiftelser och Gåvor, the Albert Påhlsson Research Foundation, and the Crafoord Foundation.

REFERENCES

1. Iselius L, Lindsten J, Morton NE, Efendic S, Cerasi E, Haegermark A, Luft R: Genetic regulation of the kinetics of glucose-induced insulin release in man: studies in families with diabetic and non-diabetic probands. *Clin Genet* 28:8–15, 1985
2. Lehtovirta M, Kaprio J, Forsblom C, Eriksson J, Tuomilehto J, Groop L: Insulin sensitivity and insulin secretion in monozygotic and dizygotic twins. *Diabetologia* 43:285–293, 2000
3. Poulsen P, Levin K, Petersen I, Christensen K, Beck-Nielsen H, Vaag A: Heritability of insulin secretion, peripheral and hepatic insulin action, and intracellular glucose partitioning in young and old Danish twins. *Diabetes* 54:275–283, 2005
4. Medici F, Hawa M, Ianari A, Pyke DA, Leslie RD: Concordance rate for type II diabetes mellitus in monozygotic twins: actuarial analysis. *Diabetologia* 42:146–150, 1999
5. Poulsen P, Kyvik KO, Vaag A, Beck-Nielsen H: Heritability of type II (non-insulin-dependent) diabetes mellitus and abnormal glucose tolerance—a population-based twin study. *Diabetologia* 42:139–145, 1999
6. Goto Y, Kakizaki M, Masaki N: Production of spontaneously diabetic rats by repetition of selective breeding. *Tohoku J Exp Med* 119:85–90, 1976
7. Suzuki K, Goto Y, Toyota T: Spontaneously diabetic GK (Goto-Kakizaki) rats. In *Lessons from Animal Diabetes*. Shafrir E, Ed. London, Smith-Gordon and Company, 1992, p. 107–116
8. Galli J, Li LS, Glaser A, Ostenson CG, Jiao H, Fakhrai-Rad H, Jacob HJ, Lander ES, Luthman H: Genetic analysis of non-insulin dependent diabetes mellitus in the GK rat. *Nat Genet* 12:31–37, 1996
9. Gauguier D, Froguel P, Parent V, Bernard C, Bihoreau MT, Portha B, James MR, Penicaud L, Lathrop M, Ktorza A: Chromosomal mapping of genetic loci associated with non-insulin dependent diabetes in the GK rat. *Nat Genet* 12:38–43, 1996
10. Galli J, Fakhrai-Rad H, Kamel A, Marcus C, Norgren S, Luthman H: Pathophysiological and genetic characterization of the major diabetes locus in GK rats. *Diabetes* 48:2463–2470, 1999
11. Lin JM, Ortsater H, Fakhrai-Rad H, Galli J, Luthman H, Bergsten P: Phenotyping of individual pancreatic islets locates genetic defects in stimulus secretion coupling to *Niddm1i* within the major diabetes locus in GK rats. *Diabetes* 50:2737–2743, 2001
12. Duggirala R, Blangero J, Almasy L, Dyer TD, Williams KL, Leach RJ, O'Connell P, Stern MP: Linkage of type 2 diabetes mellitus and of age at onset to a genetic location on chromosome 10q in Mexican Americans. *Am J Hum Genet* 64:1127–1140, 1999
13. Kim JH, Sen S, Avery CS, Simpson E, Chandler P, Nishina PM, Churchill GA, Naggert JK: Genetic analysis of a new mouse model for non-insulin-dependent diabetes. *Genomics* 74:273–286, 2001
14. Reynisdottir I, Thorleifsson G, Benediktsson R, Sigurdsson G, Emilsson V, Einarsdottir AS, Hjorleifsdottir EE, Orlygsdottir GT, Bjornsdottir GT, Saemundsdottir J, Halldorsson S, Hrafnkelsdottir S, Sigurjonsdottir SB, Steinsdottir S, Martin M, Kochan JP, Rhees BK, Grant SF, Frigge ML, Kong A, Gudnason V, Stefansson K, Gulcher JR: Localization of a susceptibility gene for type 2 diabetes to chromosome 5q34–q35.2. *Am J Hum Genet* 73:323–335, 2003
15. Clee SM, Yandell BS, Schueler KM, Rabaglia ME, Richards OC, Raines SM, Kabara EA, Klass DM, Mui ET, Stapleton DS, Gray-Keller MP, Young MB, Stoehr JP, Lan H, Boronenkov I, Raess PW, Flowers MT, Attie AD: Positional cloning of Sorcs1, a type 2 diabetes quantitative trait locus. *Nat Genet* 38:688–693, 2006
16. Grant SF, Thorleifsson G, Reynisdottir I, Benediktsson R, Manolescu A, Sainz J, Helgason A, Stefansson H, Emilsson V, Helgadottir A, Styrkarsdottir U, Magnusson KP, Walters GB, Palsdottir E, Jonsdottir T, Gudmundsdottir T, Gylfason A, Saemundsdottir J, Wilensky RL, Reilly MP, Rader DJ, Bagger Y, Christiansen C, Gudnason V, Sigurdsson G, Thorsteinsdottir U, Gulcher JR, Kong A, Stefansson K: Variant of transcription factor 7-like 2 (TCF7L2) gene confers risk of type 2 diabetes. *Nat Genet* 38:320–323, 2006
17. Fakhrai-Rad H, Nikoshkov A, Kamel A, Fernström M, Zierath JR, Norgren S, Luthman H, Galli J: Insulin-degrading enzyme identified as a candidate diabetes susceptibility gene in GK rats. *Hum Mol Genet* 14:2149–2158, 2000
18. Eliasson L, Renstrom E, Ding WG, Proks P, Rorsman P: Rapid ATP-dependent priming of secretory granules precedes Ca(2+)-induced exocytosis in mouse pancreatic B-cells. *J Physiol* 503:399–412, 1997
19. Hiriart M, Matteson DR: Na channels and two types of Ca channels in rat pancreatic B cells identified with the reverse hemolytic plaque assay. *J Gen Physiol* 91:617–639, 1988
20. Gopel S, Kanno T, Barg S, Galvanovskis J, Rorsman P: Voltage-gated and resting membrane currents recorded from B-cells in intact mouse pancreatic islets. *J Physiol* 521:717–728, 1999
21. Duchen MR, Smith PA, Ashcroft FM: Substrate-dependent changes in mitochondrial function, intracellular free calcium concentration and membrane channels in pancreatic beta-cells. *Biochem J* 294:35–42, 1993
22. Rorsman P, Renstrom E: Insulin granule dynamics in pancreatic beta cells. *Diabetologia* 46:1029–1045, 2003
23. Shih DQ, Stoffel M: Molecular etiologies of MODY and other early-onset forms of diabetes. *Curr Diab Rep* 2:125–134, 2002
24. Turner RC: The U.K. Prospective Diabetes Study: a review. *Diabetes Care* 21 (Suppl. 3):C35–C38, 1998
25. Blom T, Franzen A, Heinegard D, Holmdahl R: Comment on "The influence of the proinflammatory cytokine, osteopontin, on autoimmune demyelinating disease." *Science* 299:1845, 2003
26. Salehi A, Henningsson R, Mosen H, Ostenson CG, Efendic S, Lundquist I: Dysfunction of the islet lysosomal system conveys impairment of glucose-induced insulin release in the diabetic GK rat. *Endocrinology* 140:3045–3053, 1999
27. Clark A, Jones LC, de Koning E, Hansen BC, Matthews DR: Decreased insulin secretion in type 2 diabetes: a problem of cellular mass or function? *Diabetes* 50 (Suppl. 1):S169–S171, 2001
28. Weir GC, Bonner-Weir S: Five stages of evolving β-cell dysfunction during progression to diabetes. *Diabetes* 53 (Suppl. 3):S16–S21, 2004

29. Butler AE, Janson J, Bonner-Weir S, Ritzel R, Rizza RA, Butler PC: β-Cell deficit and increased β-cell apoptosis in humans with type 2 diabetes. *Diabetes* 52:102–110, 2003
30. McCarthy MI: Growing evidence for diabetes susceptibility genes from genome scan data. *Curr Diab Rep* 3:159–167, 2003
31. Turner MD, Cassell PG, Hitman GA: Calpain-10: from genome search to function. *Diabetes Metab Res Rev* 21:505–514, 2005
32. Schwanstecher C, Meyer U, Schwanstecher M: K(IR)6.2 polymorphism predisposes to type 2 diabetes by inducing overactivity of pancreatic beta-cell ATP-sensitive K^+ channels. *Diabetes* 51:875–879, 2002
33. Laukkanen O, Pihlajamaki J, Lindstrom J, Eriksson J, Valle TT, Hamalainen H, Ilanne-Parikka P, Keinanen-Kiukaanniemi S, Tuomilehto J, Uusitupa M, Laakso M: Polymorphisms of the SUR1 (ABCC8) and Kir6.2 (KCNJ11) genes predict the conversion from impaired glucose tolerance to type 2 diabetes: the Finnish Diabetes Prevention Study. *J Clin Endocrinol Metab* 89:6286–6290, 2004
34. Reis AF, Hani EH, Beressi N, Robert JJ, Bresson JL, Froguel P, Velho G: Allelic variation in exon 18 of the sulfonylurea receptor 1 (SUR1) gene, insulin secretion and insulin sensitivity in nondiabetic relatives of type 2 diabetic subjects. *Diabetes Metab* 28:209–215, 2002